2007

A novel class of metal-directed supramolecular DNA-delivery systems

Juan C Noveron, *University of Texas at El Paso*

A novel class of metal-directed supramolecular DNA-delivery systems†

Itzia Cruz-Campa,[a] Alejandro Arzola,[a] Lynn Santiago,[a] Jason G. Parsons,[a] Armando Varela-Ramirez,[b] Renato J. Aguilera[b] and Juan C. Noveron*[a]

Received (in Austin, TX, USA) 2nd March 2007, Accepted 19th April 2007
First published as an Advance Article on the web 9th May 2007
DOI: 10.1039/b703201c

The bis-complexes $[Cu(L_{dt})_2](OTf)_2$ (1) and $[Cu(L_{ot})_2](OTf)_2$ (2), where L_{dt} = 1-dodecyl-1,4,7-triazacyclononane, L_{ot} = 1-octadecyl-1,4,7-triazacyclononane and OTf = trifluoromethanesulfonate, formed a novel class of metallo-liposomes in water that transfect pEGFP-N1 plasmids into HEK 293-T cells at 38% and 4% efficiency, respectively.

Synthetic materials that function as DNA-delivery systems for mammalian cells are expected to play critical roles in gene therapy.[1] They can potentially overcome the fundamental problems that viral vectors present with respect to costs and health risks, as well as avoiding the immune response that the viral vectors elicit, which diminish their effectiveness.[2] On the other hand, there needs to be improvements over synthetic delivery agents that are based on quaternary ammonium surfactants because of problems with toxicity and instability of their DNA-condensates.[1,3] This has stimulated research in the development of innovated transfection systems that provide better control over the stability and programmability of the DNA lipo-complexes, which may lead to better gene delivery systems for *in vivo* applications. Recently, several new materials have been developed with these goals in mind such as dendrimeric polyamido-amines,[4] porous silica nanoparticles,[5] and gold nanoparticles.[6] Herein we report the first examples of a new class of metal-mediated supramolecular materials that can deliver large fragments of DNA into eukaryotic cells. The molecular design consists of the formation of amphiphilic Cu(II) complexes that self-assemble into metallo-liposomes in water and condense DNA plasmids into deliverable structures programmed to react with intracellular components *via* redox- and ligand-exchanged reactions. Molecular and supramolecular characterization of the materials was carried out with X-ray crystallography, extended X-ray absorbance fine structure (EXAFS) spectroscopy, transmission electron microscopy (TEM), dynamic light scattering (DLS), and fluorescent optical microscopy. Transfection studies were carried out with pEGFP-N1 DNA (4.7 kb) plasmid, which encodes for the enhanced green fluorescent protein (EGFP), and human embryonic kidney (HEK) 293-T cells.

Natural coordination-capable lipids are present in marine bacteria[7] and other organisms,[8] where they are known to function as siderophores. These molecules have the ability to self-assemble into micelles in water and upon binding to transition metal ions, they undergo phase transitions and form metallo-liposomes.[7,9] Early uses of synthetic metallo-lipids were applied to the study of electron-transfer reactions across membranes.[10] To our knowledge, the role of metallo-liposomes as gene carrying agents is unprecedented.

In this study, we synthesized two coordination-capable lipids that form bis-complexes with Cu(II) ions, namely $[Cu(II)(L_{dt})_2](OTf)_2$ (**1**) and $[Cu(II)(L_{ot})_2](OTf)_2$ (**2**), where L_{dt} = 1-dodecyl-1,4,7-triazacyclononane, L_{ot} = 1-octadecyl-1,4,7-triazacyclononane, and OTf = trifluoromethanesulfonate, Fig. 1. The non-amphiphilic model system $[Cu(II)(L_{tacn})_2](OTf)_2$ (**3**), where L_{tacn} = 1,4,7-triazacyclononane, was prepared in order to support the characterization analysis of **1** and **2**.

The ligands were prepared from the corresponding nucleophilic addition of one equivalent of 1-bromoalkane to 1,4,7-triazacyclononane (L_{tacn}) in dry THF over sodium hydride at 60 °C for 12 h. After flash column purification, they were reacted with half equivalents of $Cu(OTf)_2$ in acetonitrile at room temperature to form the corresponding amphiphilic Cu-complexes **1** and **2**, which were isolated by fractional crystallization with diethyl ether at −40 °C (~75% yield).

The corresponding non-amphiphilic Cu-complex **3** was obtained under the same reactions conditions, except by using the unmodified tacn ligand. Single-crystals suitable for X-ray diffraction analysis were obtained from diethyl ether diffusion into a concentrated CH_3CN solution of the complex at room temperature. The molecular structure of **3** is shown in Fig. 1. Cu-complex **3** crystallized in the trigonal crystal system with the $P3_121$ space group.‡ The structure reveals that the Cu atom lies on a twofold axis and is coordinated to two tacn units in an octahedral configuration with equatorial Cu–N distances of 2.053(2) and

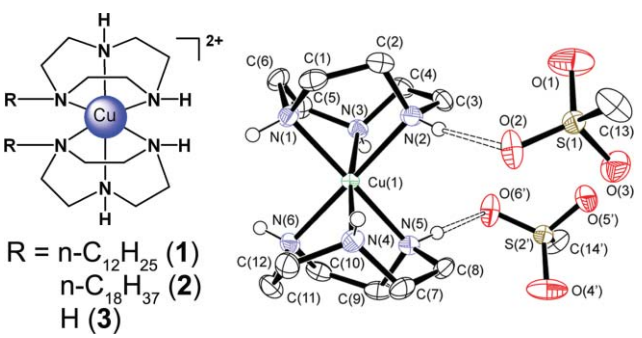

Fig. 1 ORTEP drawing for $[Cu(L_{tacn})_2](OTf)_2$ (**3**) with ellipsoids drawn at 50% probability levels. F atoms omitted for clarity.

[a]*Department of Chemistry, University of Texas, El Paso, TX, 79968, USA. E-mail: jcnoveron@utep.edu; Fax: +1 (915) 747-5748; Tel: +1 (915) 747-7572*
[b]*Department of Biological Sciences, University of Texas, El Paso, TX, 79968, USA*

† Electronic supplementary information (ESI) available: Detailed synthesis and characterization of complexes **1**, **2** and **3**, and crystallographic files for **3**. See DOI: 10.1039/b703201c

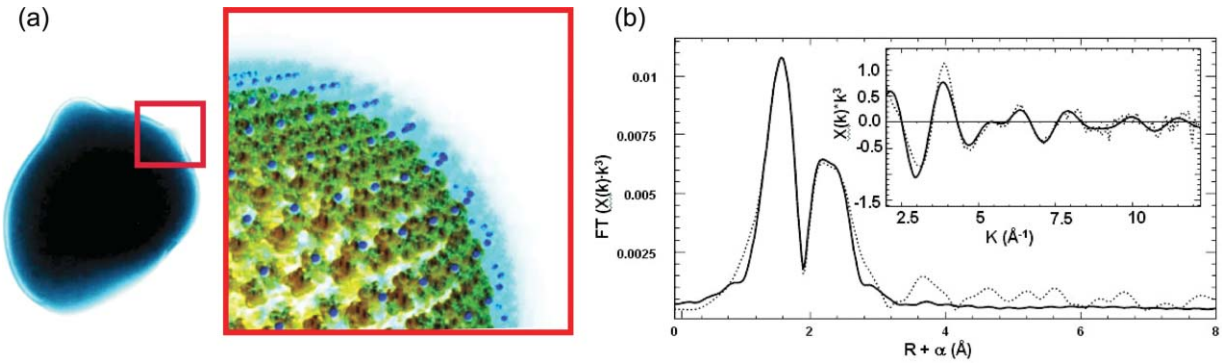

Fig. 2 (a) TEM image (color enhanced for clarity) of unilamellar metallo-liposomes of **2** and a computer model of their surface structure. (b) Fourier transform of experimental EXAFS oscillations (black line) and simulation (dashed line) of **2**.

2.075(2) Å and an axial Cu–N distance of 2.338(2) Å. The Cu-complex **3** exhibits hydrogen-bonding interactions (~2.1 Å) with the $^{-}$OTf anions with bond angles of approximately 160°.

The amphiphilic complexes **1** and **2** self-assemble into metallo-liposomes in water and exhibit an intrinsic affinity to bind the PO_4 groups of DNA *via* electrostatic and hydrogen-bonding interactions, possibly *via* similar interactions to those observed between complex **3** and $^{-}$OTf anions.

The metallo-liposomes were produced by the reverse phase methodology previously established.[11] Water was added to chloroform solutions of the complexes ($CHCl_3$: H_2O 1 : 100 v/v) and the dispersion was sonicated for 15 minutes while the organic solvent was removed in vacuum. The final volume was adjusted with water to produce 1 mM solutions. The solutions were then forced through a 0.4 μm pore-size polycarbonate filter using an extruder apparatus (Avanti Polar Lipids). The size of the metallo-liposomes was verified from DLS, which showed a narrow distribution near the pore size of the filter (400 nm). TEM analysis corroborated the size of the metallo-liposomes and revealed that their membrane had a lipid bilayer composition. EXAFS spectroscopy of the vesicles was most consistent with six N atoms as the coordination sphere of the Cu(II) center, of which two exhibit Jahn–Teller distortions, Fig. 2. Similar EXAFS data from complex **3** further confirmed this coordination structure on the surface of the metallo-liposomes.

The critical micelle concentration (cmc) values for **1** and **2** were determined using fluorescent spectroscopy,[12] and the obtained results were 50 μM and 800 μM, respectively (supporting information†). This difference may be attributed to the presence of more London dispersion forces in **2**, which may stabilize the lamellar phase that precedes vesicle formation.

The metallo-liposomes derived from **1** and **2** exhibited the ability to bind and condense the pEGFP-N1 DNA plasmid. Two DNA-condensates were observed in solution. TEM imaging revealed the formation of spherical multi-lamellar metallo-liposomes of 500 nm in diameter. Fluorescent optical microscopy on SYBR-Green stained samples revealed that double-stranded DNA is encapsulated within the spherical and multi-liposomal ensembles, Fig. 3.

The transfection ability of these DNA-condensates was tested using HEK 293-T cells and the transfection efficiency was determined to be 37% ± 4 for **1** and 4% ± 3 for **2**, Fig. 4. Solutions of complex **3** or metal-precluded solutions of **1** or **2** in EDTA-containing media showed no observable transfection.

Interestingly, the transfection efficiency of **1** is comparable with the transfection ability of some commercial liposomal transfection agents such as transfectin (Bio-Rad Laboratories), which suggests

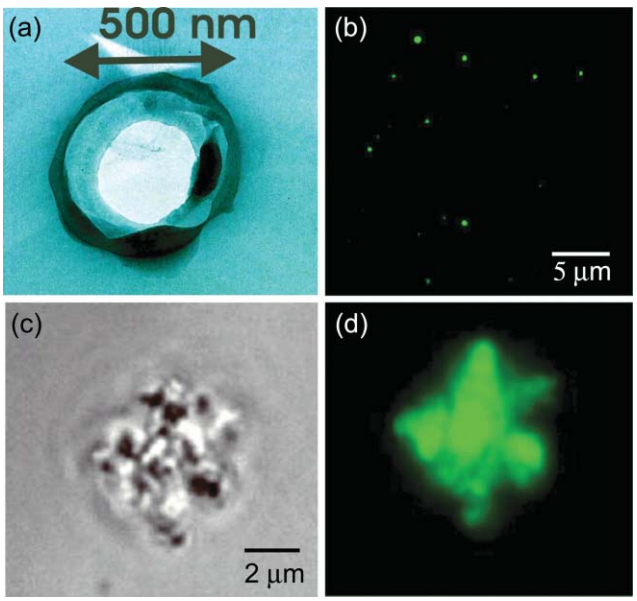

Fig. 3 (a) TEM image of spherical multi-lamellar phase condensates of pEGFP-N1 and metallo-vesicles of **2**. (b) Fluorescent light micrograph of (a) stained with SYBR-Green. (c) Bright field light micrograph of largest observable DNA condensate with metallo-liposomes of **1**. (d) Fluorescent micrograph of (c) stained with SYBR-Green.

Fig. 4 Overlays of bright field light and fluorescent light micrographs of HEK 293-T cells transfected with pEGFP-N1 DNA plasmid *via* the Cu-complex **1** (left) and Cu-complex **2** (right).

that under optimal conditions related to cell- and plasmid-types the transfection ability of **1** and **2** may be higher.

The intracellular mechanism of DNA release by the Cu-complexes is not yet known. However, given the fact that Cu-complex **3** exhibits an irreversible reduction potential of −940 mV in acetonitrile,[13] redox and ligand-exchange reactions are likely to occur during transfection, particularly in intracellular reducing environments that exist along ubiquitous mechanisms for metal regulation. The released metal ions may also play a role during transfection, as evident from recent reports of DNase II deactivation in the presence of transition metals.[14] Future designs that fine-tune the redox potential and ligand exchange kinetics of metallo-liposomes could exploit these new avenues for gene delivery.

In conclusion, we report the first example of a metal-mediated gene transfection system. The transfection ability of the Cu-complexes was associated to their cmc values, with the compound having the lowest cmc exhibiting the greatest transfection efficiency. Current studies to understand the role of the metals and to investigate structure–function relationships related to transfection ability are ongoing.

The financial support from the Lizanell & Colbert Coldwell Foundation, the NIH Grants S06 GM8012-36, 2G12RR08124, the NSF Grants 0245071 and 0649020, and the UTEP-SEED Grant are gratefully acknowledged. L. S. was supported by the RISE program (R25 GM069621-04) at UTEP. We thank Dr. Atta M. Arif for crystallographic data analysis. Synchrotron radiation experiments were performed at the Stanford Synchrotron Radiation Laboratory, Proposal #2983 M.

Notes and references

‡ CCDC 638805. For crystallographic data in CIF or other electronic format see DOI: 10.1039/b703201c

1 (*a*) D. Luo and W. M. Saltzman, *Nat. Biotechnol.*, 2000, **18**, 33; (*b*) G. Borchard, *Adv. Drug Delivery Rev.*, 2001, **52**, 145; (*c*) R. Kircheis, L. Wightman and E. Wagner, *Adv. Drug Delivery Rev.*, 2001, **53**, 341; (*d*) T. Niidome and L. Huang, *Gene Ther.*, 2002, **9**, 1647; (*e*) K. Anwer, B. G. Rhee and S. K. Mendiratta, *Crit. Rev. Ther. Drug Carrier Syst.*, 2003, **20**, 249; (*f*) M. Stefanidakis and E. Koivunen, *Curr. Pharm. Des.*, 2004, **10**, 3033; (*g*) R. I. Mahato, *Adv. Drug Delivery Rev.*, 2005, **57**, 699; (*h*) V. V. Kumar, R. S. Singh and A. Chaudhuri, *Curr. Med. Chem.*, 2003, **10**, 1297–1306.

2 (*a*) P. D. Robbins, H. Tahara and S. C. Ghivizzani, *Trends Biotechnol.*, 1998, **16**, 35–40; (*b*) E. Marshall, *Science*, 2000, **287**, 565–567.

3 (*a*) D. R. Radu, C. Y. Lai, K. Jeftinija, E. W. Rowe, S. Jeftinija and V. S.-Y. A. Lin, *J. Am. Chem. Soc.*, 2004, **126**, 13216; (*b*) P. L. Felgner, T. R. Gadek, M. Holm, R. Roman, H. W. Chan, M. Wenz, J. P. Northrop, G. M. Ringold and M. Danielsen, *Proc. Natl. Acad. Sci. U. S. A.*, 1987, **84**, 7413; (*c*) M. A. Zanta, P. Belguise-Valladier and J. P. Behr, *Proc. Natl. Acad. Sci. U. S. A.*, 1999, **96**, 91; (*d*) B. Brissault, A. Kichler, C. Guis, C. Leborgne, O. Danos and H. Cheradame, *Bioconjugate Chem.*, 2003, **14**, 581.

4 (*a*) Y. B. Lim, S. M. Kim, H. Suh and J. S. Park, *Bioconjugate Chem.*, 2002, **13**, 952; (*b*) J. Dennig and E. Duncan, *Rev. Mol. Biotechnol.*, 2002, **90**, 339.

5 (*a*) D. Luo and W. M. Saltzman, *Nat. Biotechnol.*, 2000, **18**, 893; (*b*) C. Kneuer, M. Sameti, U. Bakowsky, T. Schiestel, H. Schirra, H. Schmidt and C.-M. Lehr, *Bioconjugate Chem.*, 2000, **11**, 926; (*c*) X.-X. He, K. Wang, W. Tan, B. Liu, X. Lin, C. He, D. Li, S. Huang and J. Li, *J. Am. Chem. Soc.*, 2003, **125**, 7168–7169; (*d*) D. Luo, E. Han, N. Belcheva and W. M. Saltzman, *J. Controlled Release*, 2004, **95**, 333.

6 K. K. Sandhu, C. M. McIntosh, J. M. Simard, S. W. Smith and V. M. Rotello, *Bioconjugate Chem.*, 2002, **13**, 3.

7 (*a*) J. S. Martinez, G. P. Zhang, P. D. Holt, H.-T. Jung, C. J. Carrano, M. G. Haygood and A. Butler, *Science*, 2000, **287**, 1245–1247; (*b*) J. S. Martinez, J. N. Carter-Franklin, E. L. Mann, J. D. Martin, M. G. Haygood and A. Butler, *Proc. Natl. Acad. Sci. U. S. A.*, 2003, **100**, 3754–3759.

8 (*a*) G. A. Snow, *Bacteriol. Rev.*, 1970, **34**, 99; (*b*) M. Persmark, P. Pittman, J. S. Buyer, S. Schwyn, P. R. Gill and J. B. Neilands, *J. Am. Chem. Soc.*, 1993, **115**, 3950; (*c*) D. Lynch, J. O'Brien, T. Welch, P. Clarke, P. O. Cuiv, J. H. Crosa and M. O'Connell, *J. Bacteriol.*, 2001, **183**, 2576; (*d*) N. Okujo, Y. Sahahibara, T. Yoshida and S. Yamamoto, *BioMetals*, 1994, **7**, 170.

9 T. Owen, R. Pynn, J. S. Martinez and A. Butler, *Langmuir*, 2005, **21**, 12109–12114.

10 (*a*) J. Lahiri, G. D. Fate, S. B. Ungashe and J. T. Groves, *J. Am. Chem. Soc.*, 1996, **118**, 2347; (*b*) J. T. Groves and R. Neumann, *J. Am. Chem. Soc.*, 1987, **109**, 5045; (*c*) J. T. Groves and R. Neumann, *J. Am. Chem. Soc.*, 1989, **111**, 2900.

11 E. Abel, M. F. Fedders and G. W. Gokel, *J. Am. Chem. Soc.*, 1995, **117**, 1265–1270.

12 C. Lau, R. Bitton, H. Bianco-Peled, D. G. Schultz, D. J. Cookson, S. T. Grosser and J. W. Schneider, *J. Phys. Chem. B*, 2006, **110**, 9027–9033.

13 A. D. Beveridge, A. J. Lavery, M. D. Walkinshaw and M. Schröder, *J. Chem. Soc., Dalton Trans.*, 1987, 373–377.

14 E. J. Niedzinski, D. C. Olson, Y. J. Chen, J. A. Udove, M. H. Nantz, H. C. Tseng, J. L. Bolaffi and M. J. Bennett, *Mol. Ther.*, 2003, **7**, 396–400.

Supplementary Material (ESI) for Chemical Communications

Supporting Information

A novel class of metal-directed supramolecular DNA-delivery systems

Itzia Cruz-Campa[†], Alejandro Arzola[†], Lynn Santiago[†], Jason G. Parsons[†], Armando Varela-Ramirez[‡], Renato J. Aguilera[‡], and Juan C. Noveron[†]*

[†]Department of Chemistry and [‡]Department of Biological Sciences, University of Texas, El Paso, TX, 79968, USA, Fax: (915)747-5748; Tel(915) 747-7572; E-mail: jcnoveron@utep.edu

Experimental

All chemicals were used as commercially supplied. Solvents where distilled under appropriated drying agents. Infrared spectra were recorded on a Perkin-Elmer FT-IR spectrometer. NMR spectra were recorded on Varian Unity 300 or Varian XL-300 spectrometers. The ^{1}H chemical shifts are reported relative to the residual protons of the deuterated solvents. Mass spectra were obtained with a Finnigan MAT 95 mass spectrometer with a Finnigan MAT ICIS II operating system at 80 eV (EI). UV-vis spectra were recorded in the visible range (400-800 nm) on a Perkin Elmer Lambda 35 spectrometer. UV WinLab v. 2.85.04 software was used to analyze the spectra.

Synthesis of ligands L_{dt} and L_{ot}. 1-dodecyl-1,4,7-triazacyclononane (L_{dt}) and 1-octadecyl-1,4,7-triazacyclononane (L_{ot}) synthesis were performed using the same procedure. In a 25 mL Schlenk flask under an atmosphere of nitrogen, a mixture of 1,4,7-triazacyclononane (300 mg, 2.31 mmol) and 1.1 equivalents of sodium hydride (60 mg, 2.55 mmol) in 10 mL of dry THF was stirred for 10 minutes. A solution containing 1 equivalent of 1-bromododecane (688 mg, 2.31 mmol) or 1-bromooctadecane (769 mg, 2.31 mmol) was added drop by drop under a nitrogen atmosphere to the reaction flask. The reaction mixture was stirred overnight in an oil bath at 60 ºC. Solvent was removed by rotary evaporation and the solid was dissolved in chloroform. The products were isolated using an automated flash chromatography system (Biotage) using a gradient of chloroform-methanol on a silica column. 573 mg (83%) of L_{dt} were obtained as a pale yellow viscous liquid and L_{ot} was obtained as a pale yellow wax like solid, 620 mg (70%). Similar NMR and IR spectra were obtained for both compounds. IR bands (KBr pellet, cm^{-1}) 3405 (N-H), 2918, 2850, 721(C-H); ^{1}H NMR ($CDCl_3$, 300 MHz): δ 2.5-3.4 (m, -NH-C**H**), 0.8 (t, 3H, C**H**$_3$), 1.1-1.7 (m, C**H**$_2$).

Synthesis of Cu-complexes 1, 2 and 3. Amphiphilic complexes bis(1-dodecyl-1,4,7-triazacyclononane)copper(II) triflate **(1)** and bis(1-octadecyl-1,4,7-triazacyclononane) copper(II) triflate, (UV-vis λ_{max} = 640 nm in ACN) **(2)** were prepared by dissolving copper(II) trifluoromethanesulfonate, $Cu(OTf)_2$ (38 mg 0.1 mmol) in 2 mL of acetonitrile and adding 2 equivalents of L_{dt} (60 mg, 0.2 mmol) or L_{ot} (76 mg, 0.2

mmol). The solutions were stirred at room temperature under nitrogen atmosphere for 24 hours. The compounds were isolated by fractional crystallization with diethyl ether at -40 ^{o}C. Liposomes of **1** and **2** were obtained were produced by the reverse phase methodology. Water was added to chloroform solutions of the complexes ($CHCl_3$: H_2O 1:100v/v) and the dispersion was sonicated for 30 minutes while the organic solvent was removed in vacuum. The final volume was adjusted with water to produce 1mM solutions. The solutions were then forced through a 0.4 μm pore-size polycarbonate filter using an extruder apparatus (Avanti Polar Lipids). In order to synthesize bis(1,4,7-triazacyclononane)copper(II) triflate **(3)** 2 equivalents of 1,4,7- triazacyclononane (100 mg, 0.77 mmol) were dissolved in 1 mL of acetonitrile. This mixture was added dropwise to a continued stirred solution of $Cu(OTf)_2$ (140 mg, 0.38 mmol) in 1 mL of acetonitrile. UV-vis λ_{max} = 620 nm (ACN). The combined mixture turned dark blue. Blue prismatic crystals were obtained by diethyl ether diffusion into a concentrated CH_3CN solution of the complex at room temperature.

Dynamic Light Scattering. Dynamic Light Scattering determinations were performed on a PD2000 DLS Plus (Precision Detectors) at 20 °C, with a scattering angle of 90.0°. The data collected was analyzed using the software Precision Deconvolve Version 4.5. 1mM aqueous dispersions of amphiphilic Cu-complexes **1** and **2** were measured.

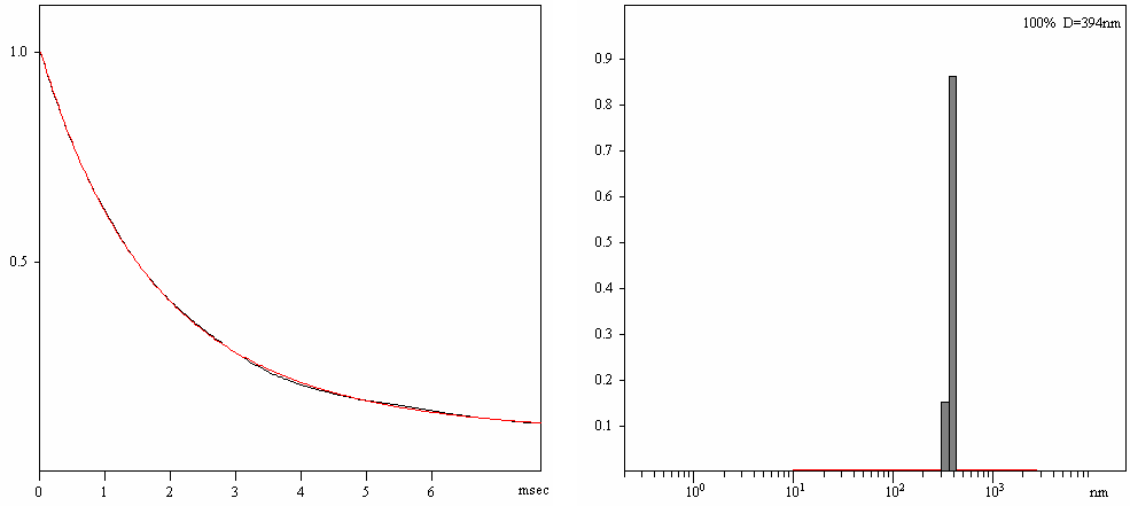

Figure S1. DLS measurement and correlation function of Cu-complex **1**

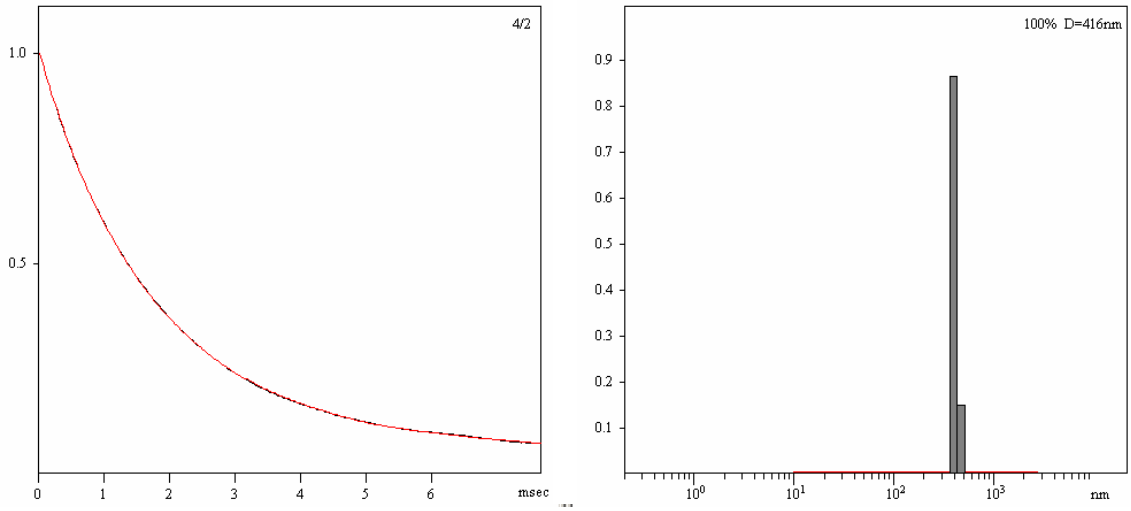

Figure S2. DLS measurement and correlation function of Cu-complex **2.**

Transmission Electron Microscopy. Samples were examined in a Hitachi H-8000 analytical transmission electron microscope. The TEM was operated at 200 kV accelerating potential. A drop of an aqueous 1 mM dispersion of Cu-complex **2** with and without DNA (pEGFP-N1) was placed over a silicon monoxide-coated 200 mesh copper grid and air evaporated.

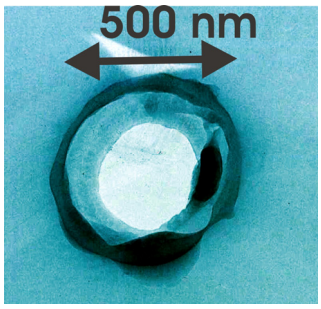

Figure S3. TEM image of Cu-complex **2** with pEGFP-N1.

Critical Micelle Concentration Determination. The critical micelle concentration for the amphiphilic complexes was determined by a dye solubilization method using the fluorescent lipophilic probe nile red[1] (Sigma Aldrich). Fluorescence intensity of nile red solutions with increasing concentration of surfactant were measured at 640 nm on a Fluoroskan microplate reader using an excitation wavelength of 530 nm. The integration time was set to 100 ms. An aqueous stock solution of nile red was prepared dissolving

400 μL of an acetone dye solution (1mg/mL) and adding water for a total volume of 10 mL. 20 μL of nile red stock solution were added in each well of a 96-well black plate for fluorescence experiments. The concentration of amphiphilic complexes was varied from 0-400 μM using a 1mM stock solution of Cu-complex **1** and from 0-1600 μM using a 4 mM stock solution of Cu-complex **2**. The total volume in each well was adjusted to 50 μL with water. The experiments were performed by triplicate.

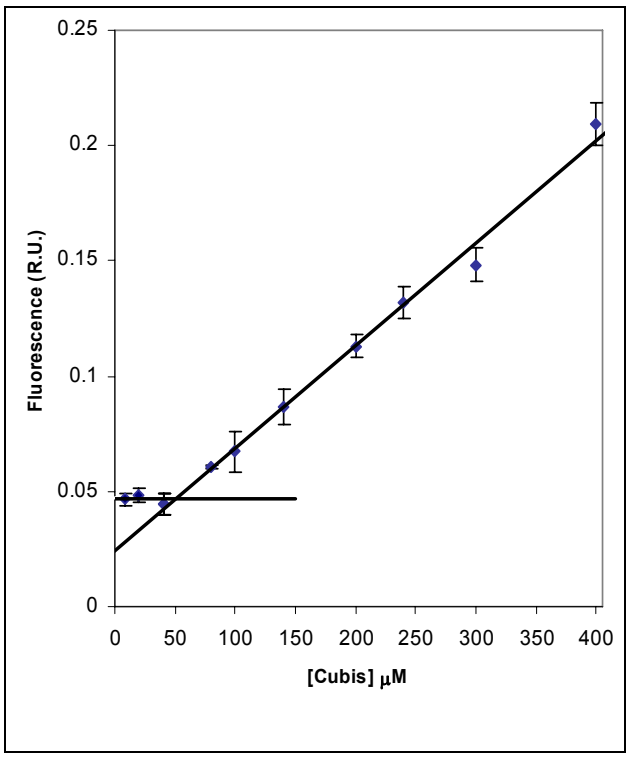

Figure S4. Determination of cmc of Cu-complex **1** (cmc= 50μM).

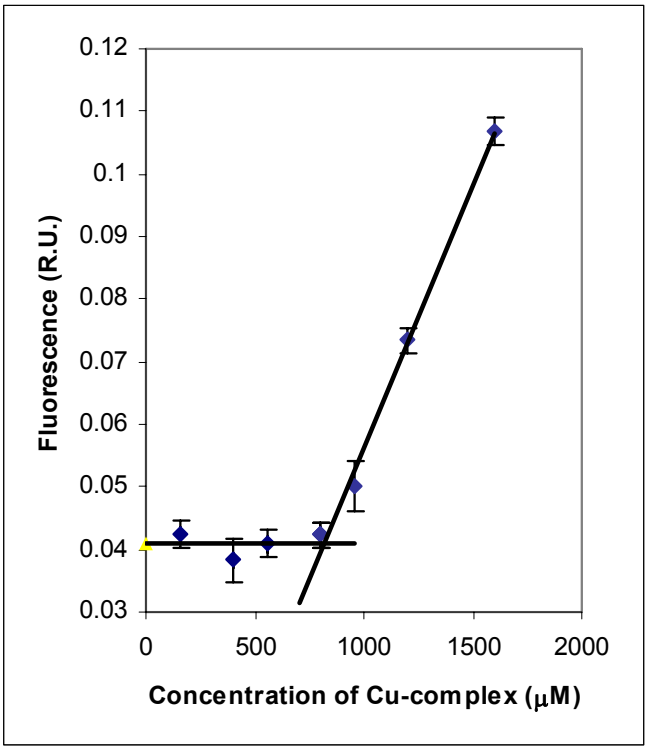

Figure S5. Determination of cmc of Cu-complex **2** (cmc= 800μM).

Transfection experiments. Human embryonic kidney (HEK) 293T cells (Edge Biosystems, Gaithersburg, MD) were cultured in Dulbbecco's modified Eagle's medium (DMEM, Mediatech, Herndon, VA) supplemented with antibiotics and 10% heat inactivated newborn calf serum (Hyclone Laboratories, Logan, UT). pEGFP-N1 green fluorescent protein-encoded plasmid (BD Clontech. Palo Alto, CA) was amplified in *Escherichia coli* and purified with Maxipreps kit (Promega. Madison, WI). Additionally, closed circular DNA plasmid was purified using equilibrium centrifugation in CsCl-ethidium bromide gradients (Sambrook, *et. al*.[2]).

HEK 293-T cells were cultured in 24-well plates at 40,000 cells/well in a total volume 1 ml of complete media, then incubated to reach about 40 to 50 % of confluence. Cells were washed with DMEM without serum previously to be transfected transiently.

DNA-liposome complexes were produced combining a diluted solutions of DNA with a diluted solution of liposomes (1 μg circular plasmid DNA in 50 μl serum free media with a 50 μL media solution containing 0.5, 1, 2, 3, 4 and 8 μL of a 1mM aqueous solution of

copper complexes **1** and **2**, respectively. After 15 min of incubation 0.4 ml of DMEM without serum were mixed with the complexes and then added to cells. Lipofectin (Invitrogen. Carlsbad, CA) was used as a positive control for transfection. After overnight incubation, wells were monitored by fluorescent microscopy to differentiate transfected (fluorescent) cells from non transfected cells. Experiments were done by triplicate. The transfection efficiency was calculated dividing the number of transfected cells over the total number of cells counted. At least 500 cells were counted by cell.

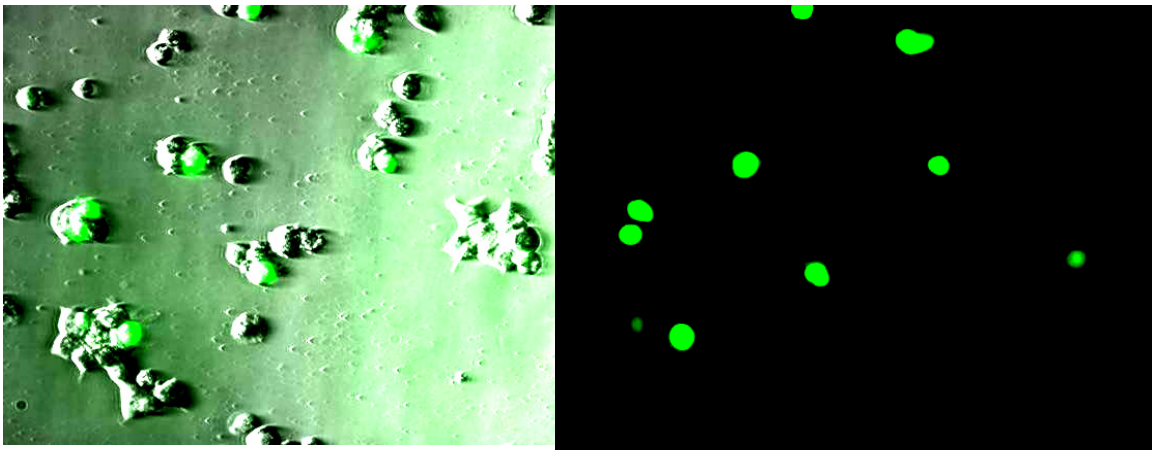

Figure S6. Optical fluorescent microscopy of transfected cells with Cu-complex 1.

Gel Electrophoresis on Cu complex 1 and pDNA.

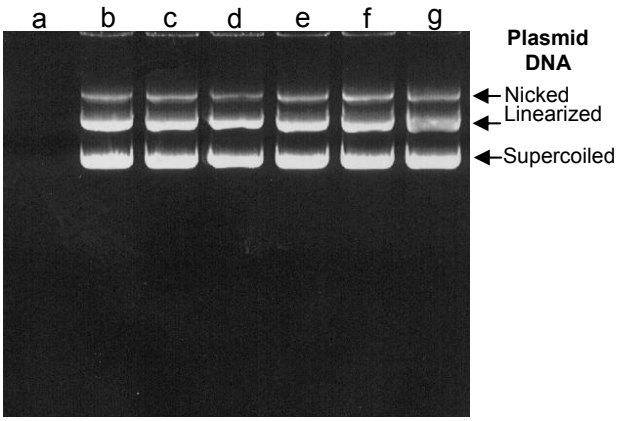

Figure S7. Reaction mixture, 20 µl total volume, containing final concentration of 500 µM of **1** in a DNase II buffer plus 1 µg of DNA pEGFP-N1 were incubated at 37ºC by **b**: 0 h, **c**: 0.5 h, **d**: 1 h, **e**: 2 h, **f**: 3 h, respectively. Two controls were included, **a**: Cu complex **1** alone and **g**: DNA pEGFP-N1 alone. Plasmid DNA integrity was analyzed, after the reaction products were separated by 1%-(w/v)-agarose-gel electrophoresis and visualized with UV-light trans-illuminator. The results demonstrated that no degradation products of DNA were observed even after a 3 h incubation time with **1**.

Single-crystal X-Ray Crystallography of Cu-complex 3. [CCDC 638805] A blue prism shaped crystal 0.33 x 0.30 x 0.13 mm in size was mounted on a glass fiber with traces of viscous oil and then transferred to a Nonius KappaCCD diffractometer equipped with Mo Kα radiation (λ = 0.71073 Å). Ten frames of data were collected at 150(1)K with an oscillation range of *1* deg/frame and an exposure time of 20 sec/frame.[3] Indexing and unit cell refinement based on all observed reflection from those ten frames, indicated a trigonal ***P*** lattice. A total of 5097 reflections (Θ_{max} = 27.48°) were indexed, integrated and corrected for Lorentz, polarization and absorption effects using DENZO-SMN and SCALEPAC.[4] Post refinement of the unit cell gave *a* = 9.4428(2) Å, b = 9.4428(2) Å, c = 24.7664(7) Å, and V = 1912.47(8) Å^3. Axial photographs and systematic absences were consistent with the compound having crystallized in the Trigonal space group ***P***3_1 2 1.

The structure was solved by a combination of direct methods and heavy atom using SIR 97.[5] All of the non-hydrogen atoms were refined with anisotropic displacement coefficients. Hydrogen atoms were assigned isotropic displacement coefficients U(H) = 1.2U(C), and their coordinates were allowed to ride on their respective carbons using SHELXL97.[6] The weighting scheme employed was $w = 1/[\sigma^2(F_o^2) + (0.0304P)^2 + 0.8643P]$ where $P = (F_o^2 + 2F_c^2)/3$. The refinement converged to R1 = 0.0324, wR2 = 0.0739, and S = 1.049 for 2726 reflections with 1> 2σ(I), and R1 = 0.0370, wR2 = 0.0765, and S = 1.049 for 2922 unique reflections and 169 parameters.[7] The maximum Δ/σ in the final cycle of the least-squares was 0.001, and the residual peaks on the final difference-Fourier map ranged from -0.323 to 0.387 e/Å^3. Scattering factors were taken from the International Tables for Crystallography, Volume C. [8, 9]

Table S1. Crystal data and structure refinement for Cu-complex 3.

Identification code	Cu complex **3**	
Empirical formula	C14 H32 Cu F6 N6 O7 S2	
Formula weight	638.12	
Temperature	150(1) K	
Wavelength	0.71073 Å	
Crystal system	Trigonal	
Space group	***P***3_1 2 1	
Unit cell dimensions	a = 9.4428(2) Å	α= 90°.

	b = 9.4428(2) Å	β= 90°.
	c = 24.7664(7) Å	γ = 120°.
Volume	1912.47(8) $Å^3$	
Z	3	
Density (calculated)	1.662 Mg/m^3	
Absorption coefficient	1.110 mm^{-1}	
F(000)	987	
Crystal size	0.33 x 0.30 x 0.13 mm^3	
Theta range for data collection	4.13 to 27.48°.	
Index ranges	-12<=h<=12, -10<=k<=10, -32<=l<=29	
Reflections collected	5097	
Independent reflections	2922 [R(int) = 0.0331]	
Completeness to theta = 27.48°	99.0 %	
Absorption correction	Multi-scan	
Max. and min. transmission	0.8691 and 0.7108	
Refinement method	Full-matrix least-squares on F^2	
Data / restraints / parameters	2922 / 0 / 169	
Goodness-of-fit on F^2	1.049	
Final R indices [I>2sigma(I)]	R1 = 0.0324, wR2 = 0.0739	
R indices (all data)	R1 = 0.0370, wR2 = 0.0765	
Absolute structure parameter	0.024(14)	
Largest diff. peak and hole	0.387 and -0.323 $e.Å^{-3}$	

Table S2. Atomic coordinates (x 10^4) and equivalent isotropic displacement parameters ($Å^2$x 10^3) for Cu complex 3. U(eq) is defined as one third of the trace of the orthogonalized U^{ij} tensor.

	x	y	z	U(eq)
Cu(1)	-575(1)	-575(1)	5000	17(1)
S(1)	-4563(1)	3389(1)	4119(1)	26(1)
F(1)	-4068(4)	2144(3)	3253(1)	83(1)
F(2)	-2090(3)	4470(5)	3465(1)	107(1)
F(3)	-4258(3)	4250(3)	3106(1)	63(1)
O(1)	-6287(2)	2338(3)	4015(1)	42(1)
O(2)	-3817(4)	2693(4)	4440(1)	62(1)
O(3)	-4138(3)	5020(3)	4264(1)	46(1)

O(4)	-8635(3)	0	3333	34(1)
N(1)	-1006(2)	101(2)	4131(1)	23(1)
N(2)	-76(3)	1806(2)	5118(1)	24(1)
N(3)	-2960(2)	-1125(3)	5084(1)	25(1)
C(1)	-517(3)	1846(3)	4132(1)	28(1)
C(2)	576(3)	2734(3)	4613(1)	27(1)
C(3)	-1575(3)	1791(3)	5318(1)	29(1)
C(4)	-2861(3)	71(4)	5490(1)	30(1)
C(5)	-3727(3)	-1048(3)	4566(1)	29(1)
C(6)	-2770(3)	-1043(3)	4069(1)	29(1)
C(7)	-3676(4)	3612(4)	3450(1)	44(1)

Table S3. Bond lengths [Å] and angles [°] for Cu complex 3.

Cu(1)-N(3)#1	2.053(2)
Cu(1)-N(3)	2.053(2)
Cu(1)-N(2)	2.075(2)
Cu(1)-N(2)#1	2.075(2)
Cu(1)-N(1)	2.3377(19)
Cu(1)-N(1)#1	2.3378(19)
S(1)-O(2)	1.422(2)
S(1)-O(3)	1.428(2)
S(1)-O(1)	1.444(2)
S(1)-C(7)	1.821(3)
F(1)-C(7)	1.336(4)
F(2)-C(7)	1.299(4)
F(3)-C(7)	1.312(4)
O(4)-H(4)	0.86(3)
N(1)-C(6)	1.471(3)
N(1)-C(1)	1.473(3)
N(1)-H(1)	0.9300
N(2)-C(2)	1.475(3)
N(2)-C(3)	1.492(3)
N(2)-H(2)	0.9300
N(3)-C(4)	1.481(3)

N(3)-C(5)	1.491(3)
N(3)-H(3)	0.9300
C(1)-C(2)	1.523(4)
C(1)-H(1A)	0.9900
C(1)-H(1B)	0.9900
C(2)-H(2A)	0.9900
C(2)-H(2B)	0.9900
C(3)-C(4)	1.524(4)
C(3)-H(3A)	0.9900
C(3)-H(3B)	0.9900
C(4)-H(4A)	0.9900
C(4)-H(4B)	0.9900
C(5)-C(6)	1.526(4)
C(5)-H(5A)	0.9900
C(5)-H(5B)	0.9900
C(6)-H(6A)	0.9900
C(6)-H(6B)	0.9900

N(3)#1-Cu(1)-N(3)	95.10(12)
N(3)#1-Cu(1)-N(2)	177.36(9)
N(3)-Cu(1)-N(2)	83.45(8)
N(3)#1-Cu(1)-N(2)#1	83.45(8)
N(3)-Cu(1)-N(2)#1	177.36(9)
N(2)-Cu(1)-N(2)#1	98.08(12)
N(3)#1-Cu(1)-N(1)	102.92(8)
N(3)-Cu(1)-N(1)	80.98(8)
N(2)-Cu(1)-N(1)	79.06(8)
N(2)#1-Cu(1)-N(1)	97.18(8)
N(3)#1-Cu(1)-N(1)#1	80.97(8)
N(3)-Cu(1)-N(1)#1	102.92(8)
N(2)-Cu(1)-N(1)#1	97.18(8)
N(2)#1-Cu(1)-N(1)#1	79.06(8)
N(1)-Cu(1)-N(1)#1	174.33(10)
O(2)-S(1)-O(3)	114.96(16)
O(2)-S(1)-O(1)	115.50(17)
O(3)-S(1)-O(1)	113.47(14)

O(2)-S(1)-C(7)	104.77(14)
O(3)-S(1)-C(7)	103.75(16)
O(1)-S(1)-C(7)	102.27(13)
C(6)-N(1)-C(1)	115.4(2)
C(6)-N(1)-Cu(1)	100.58(14)
C(1)-N(1)-Cu(1)	107.66(14)
C(6)-N(1)-H(1)	110.9
C(1)-N(1)-H(1)	110.9
Cu(1)-N(1)-H(1)	110.9
C(2)-N(2)-C(3)	113.6(2)
C(2)-N(2)-Cu(1)	108.98(15)
C(3)-N(2)-Cu(1)	109.61(15)
C(2)-N(2)-H(2)	108.2
C(3)-N(2)-H(2)	108.2
Cu(1)-N(2)-H(2)	108.2
C(4)-N(3)-C(5)	113.2(2)
C(4)-N(3)-Cu(1)	103.47(15)
C(5)-N(3)-Cu(1)	113.51(15)
C(4)-N(3)-H(3)	108.8
C(5)-N(3)-H(3)	108.8
Cu(1)-N(3)-H(3)	108.8
N(1)-C(1)-C(2)	111.41(19)
N(1)-C(1)-H(1A)	109.3
C(2)-C(1)-H(1A)	109.3
N(1)-C(1)-H(1B)	109.3
C(2)-C(1)-H(1B)	109.3
H(1A)-C(1)-H(1B)	108.0
N(2)-C(2)-C(1)	111.7(2)
N(2)-C(2)-H(2A)	109.3
C(1)-C(2)-H(2A)	109.3
N(2)-C(2)-H(2B)	109.3
C(1)-C(2)-H(2B)	109.3
H(2A)-C(2)-H(2B)	107.9
N(2)-C(3)-C(4)	110.5(2)
N(2)-C(3)-H(3A)	109.6
C(4)-C(3)-H(3A)	109.6

N(2)-C(3)-H(3B)	109.6
C(4)-C(3)-H(3B)	109.6
H(3A)-C(3)-H(3B)	108.1
N(3)-C(4)-C(3)	109.6(2)
N(3)-C(4)-H(4A)	109.8
C(3)-C(4)-H(4A)	109.8
N(3)-C(4)-H(4B)	109.8
C(3)-C(4)-H(4B)	109.8
H(4A)-C(4)-H(4B)	108.2
N(3)-C(5)-C(6)	113.1(2)
N(3)-C(5)-H(5A)	109.0
C(6)-C(5)-H(5A)	109.0
N(3)-C(5)-H(5B)	109.0
C(6)-C(5)-H(5B)	109.0
H(5A)-C(5)-H(5B)	107.8
N(1)-C(6)-C(5)	111.6(2)
N(1)-C(6)-H(6A)	109.3
C(5)-C(6)-H(6A)	109.3
N(1)-C(6)-H(6B)	109.3
C(5)-C(6)-H(6B)	109.3
H(6A)-C(6)-H(6B)	108.0
F(2)-C(7)-F(3)	110.4(3)
F(2)-C(7)-F(1)	107.0(3)
F(3)-C(7)-F(1)	106.0(3)
F(2)-C(7)-S(1)	111.5(2)
F(3)-C(7)-S(1)	111.7(2)
F(1)-C(7)-S(1)	109.9(2)

Symmetry transformations used to generate equivalent atoms:

#1 y,x,-z+1

Table S4. Anisotropic displacement parameters ($Å^2 x\ 10^3$)for Cu complex 3. The anisotropic displacement factor exponent takes the form: $-2\pi^2[\ h^2 a^{*2} U^{11} + ... + 2\ h\ k\ a^*\ b^*\ U^{12}\ ]$

	U^{11}	U^{22}	U^{33}	U^{23}	U^{13}	U^{12}

Cu(1)	17(1)	17(1)	20(1)	1(1)	-1(1)	10(1)
S(1)	25(1)	25(1)	28(1)	2(1)	-1(1)	13(1)
F(1)	115(2)	107(2)	64(1)	-20(1)	11(1)	84(2)
F(2)	30(1)	194(3)	59(1)	4(2)	10(1)	29(2)
F(3)	66(1)	81(2)	39(1)	22(1)	-1(1)	34(1)
O(1)	28(1)	37(1)	38(1)	-5(1)	4(1)	0(1)
O(2)	87(2)	88(2)	45(1)	15(1)	-4(1)	69(2)
O(3)	47(1)	29(1)	56(1)	-13(1)	-14(1)	15(1)
O(4)	30(1)	43(2)	35(1)	-13(1)	-6(1)	22(1)
N(1)	26(1)	24(1)	22(1)	1(1)	2(1)	14(1)
N(2)	26(1)	24(1)	26(1)	0(1)	-1(1)	15(1)
N(3)	19(1)	27(1)	28(1)	6(1)	4(1)	11(1)
C(1)	35(2)	25(1)	28(1)	10(1)	4(1)	17(1)
C(2)	30(1)	18(1)	32(1)	4(1)	3(1)	11(1)
C(3)	35(2)	33(1)	28(1)	-3(1)	-1(1)	25(1)
C(4)	31(1)	43(2)	26(1)	2(1)	4(1)	26(1)
C(5)	20(1)	34(1)	30(1)	4(1)	-4(1)	12(1)
C(6)	28(1)	31(1)	24(1)	1(1)	-6(1)	12(1)
C(7)	34(2)	67(2)	36(1)	4(1)	1(1)	29(2)

Table S5. Hydrogen coordinates (x 10^4) and isotropic displacement parameters ($Å^2$x 10^3) for Cu complex 3.

	x	y	z	U(eq)
H(4)	-7740(40)	700(40)	3483(14)	46(10)
H(1)	-409	-111	3877	28
H(2)	728	2283	5382	29
H(3)	-3567	-2172	5226	30
H(1A)	-1506	1954	4146	34
H(1B)	74	2360	3794	34
H(2A)	1685	2903	4546	33
H(2B)	672	3822	4651	33
H(3A)	-2023	2177	5029	34

H(3B)	-1289	2545	5629	34
H(4A)	-2568	-185	5846	36
H(4B)	-3938	4	5524	36
H(5A)	-3812	-45	4564	34
H(5B)	-4849	-1999	4546	34
H(6A)	-2955	-2160	4008	35
H(6B)	-3177	-730	3748	35

Table S6. Torsion angles [°] for Cu complex 3.

N(3)#1-Cu(1)-N(1)-C(6)	63.36(15)
N(3)-Cu(1)-N(1)-C(6)	-29.84(15)
N(2)-Cu(1)-N(1)-C(6)	-114.86(15)
N(2)#1-Cu(1)-N(1)-C(6)	148.25(15)
N(1)#1-Cu(1)-N(1)-C(6)	-163.65(14)
N(3)#1-Cu(1)-N(1)-C(1)	-175.51(15)
N(3)-Cu(1)-N(1)-C(1)	91.29(16)
N(2)-Cu(1)-N(1)-C(1)	6.27(15)
N(2)#1-Cu(1)-N(1)-C(1)	-90.62(16)
N(1)#1-Cu(1)-N(1)-C(1)	-42.52(14)
N(3)#1-Cu(1)-N(2)-C(2)	-168.9(19)
N(3)-Cu(1)-N(2)-C(2)	-112.03(17)
N(2)#1-Cu(1)-N(2)-C(2)	65.80(15)
N(1)-Cu(1)-N(2)-C(2)	-30.00(16)
N(1)#1-Cu(1)-N(2)-C(2)	145.71(16)
N(3)#1-Cu(1)-N(2)-C(3)	-44(2)
N(3)-Cu(1)-N(2)-C(3)	12.81(16)
N(2)#1-Cu(1)-N(2)-C(3)	-169.4(2)
N(1)-Cu(1)-N(2)-C(3)	94.84(17)
N(1)#1-Cu(1)-N(2)-C(3)	-89.46(16)
N(3)#1-Cu(1)-N(3)-C(4)	142.59(18)
N(2)-Cu(1)-N(3)-C(4)	-35.19(15)
N(2)#1-Cu(1)-N(3)-C(4)	-161(2)
N(1)-Cu(1)-N(3)-C(4)	-115.10(16)
N(1)#1-Cu(1)-N(3)-C(4)	60.70(16)

N(3)#1-Cu(1)-N(3)-C(5)	-94.33(18)
N(2)-Cu(1)-N(3)-C(5)	87.89(19)
N(2)#1-Cu(1)-N(3)-C(5)	-38(2)
N(1)-Cu(1)-N(3)-C(5)	7.98(17)
N(1)#1-Cu(1)-N(3)-C(5)	-176.21(17)
C(6)-N(1)-C(1)-C(2)	129.6(2)
Cu(1)-N(1)-C(1)-C(2)	18.3(2)
C(3)-N(2)-C(2)-C(1)	-71.3(3)
Cu(1)-N(2)-C(2)-C(1)	51.1(2)
N(1)-C(1)-C(2)-N(2)	-45.9(3)
C(2)-N(2)-C(3)-C(4)	134.7(2)
Cu(1)-N(2)-C(3)-C(4)	12.6(2)
C(5)-N(3)-C(4)-C(3)	-71.4(2)
Cu(1)-N(3)-C(4)-C(3)	51.9(2)
N(2)-C(3)-C(4)-N(3)	-43.7(3)
C(4)-N(3)-C(5)-C(6)	133.4(2)
Cu(1)-N(3)-C(5)-C(6)	15.8(3)
C(1)-N(1)-C(6)-C(5)	-68.9(3)
Cu(1)-N(1)-C(6)-C(5)	46.6(2)
N(3)-C(5)-C(6)-N(1)	-45.7(3)
O(2)-S(1)-C(7)-F(2)	-55.9(3)
O(3)-S(1)-C(7)-F(2)	65.0(3)
O(1)-S(1)-C(7)-F(2)	-176.8(3)
O(2)-S(1)-C(7)-F(3)	180.0(3)
O(3)-S(1)-C(7)-F(3)	-59.1(3)
O(1)-S(1)-C(7)-F(3)	59.1(3)
O(2)-S(1)-C(7)-F(1)	62.6(3)
O(3)-S(1)-C(7)-F(1)	-176.5(2)
O(1)-S(1)-C(7)-F(1)	-58.2(2)

Symmetry transformations used to generate equivalent atoms:

#1 y,x,-z+1

Table S7. Hydrogen bonds for Cu complex 3 [Å and °].

D-H...A	d(D-H)	d(H...A)	d(D...A)	<(DHA)
O(4)-H(4)...O(1)	0.86(3)	1.97(3)	2.784(2)	158(3)
N(1)-H(1)...O(4)#2	0.93	2.11	3.023(3)	166.3
N(2)-H(2)...O(1)#3	0.93	2.08	2.990(3)	167.3
N(3)-H(3)...O(3)#4	0.93	2.08	2.987(3)	163.2

Symmetry transformations used to generate equivalent atoms:

#1 y,x,-z+1 #2 x+1,y,z #3 y,x+1,-z+1 #4 y-1,x,-z+1

References

1 Lau, Cheryl; Bitton, Ronit; Bianco-Peled, Havazelet; Schultz, David G.; Cookson, David J.; Grosser, Shane T.; Schneider, James W. J. Phys. Chem. B. **2006**, *110,* 9027-9033.

2. Sambrook, J., Fritsch, E.F. & Maniatis, T.; Hrsg. *Molecular Cloning - A Laboratory Manual, 2**nd** Edition*. Cold Spring Habour Laboratory Press, **1989**, New York.

3. COLLECT Data Collection Software. Nonius B.V. **1998**.

4. Otwinowski, Z.; Minor, W., *Methods Enzymol*. **1997**, *276*, 307-326.

5. SIR97 (Release 1.02) - A program for automatic solution and refinement of crystal structure. A. Altomare, M.C. Burla, M. Camalli, G. Cascarano, C. Giacovazzo, A. Guagliardi, A.G. G. Moliteni, G. Polidori, and R. Spagna.

6. SHELX97 [Includes SHELXS97, SHELXL97, CIFTAB] - Sheldrick, G. M. (**1997**). Programs for Crystal Structure Analysis (Release 97-2). University of Göttingen, Germany.

7. $R1 = \Sigma(||F_o| - |F_c||) / \Sigma |F_o|$, $wR2 = [\Sigma(w(F_o^2 - F_c^2)2) / \Sigma(F_o^2)^2]^{1/2}$, and S = Goodness-of-fit on $F^2 = [\Sigma(w(F_o^2 - F_c^2)^2 / (n-p)]^{1/2}$, where n is the number of reflections and p is the number of parameters refined.

8. Maslen, E. N.; Fox, A. G.; O'Keefe, M. A., *International Tables for Crystallography: Mathemetical, Physical and Chemical Tables*, Vol. C, Chapter 6, Wilson, A. J. C., Ed.; Kluwer, Dordrecht, The Netherlands, **1992**;. 476-516.

9. Creagh, D. C.; McdAuley, W. J., I*nternational Tables for Crystallography: mathematical, Physical and Chemical tables*, Vol. C, Chapter 4 Wilson, A. J. C., Ed.; Kluwer, Dordrecht, The Netherlands, **1992**; 206-222.